Si/SiO$_2$ interface studies by spectroscopic immersion ellipsometry and atomic force microscopy

Q. Liu, J. F. Wall, and E. A. Irene
Department of Chemistry, University of North Carolina at Chapel Hill, Chapel Hill, North Carolina 27599-3290

The dependence of the Si/SiO$_2$ interface characteristics on the thickness and oxidation temperature for SiO$_2$ films grown on different Si orientations was studied by spectroscopic immersion ellipsometry (SIE) and atomic force microscopy (AFM). Essentially, SIE uses liquids that match the refractive index of the films, thereby optically removing the films and consequently increasing the sensitivity to the interface. We show that as the thickness of the thermally grown SiO$_2$ overlayer increases, the thickness of the suboxide layer at the interface also increases, and the average radius of the crystalline silicon protrusions (roughness) at the interface decreases for the three different Si orientations (100), (110), and (111), and two different oxidation temperatures (800 and 1000 °C) studied. The dependence of the interface roughness on the thickness of the SiO$_2$ overlayer was confirmed by AFM. The results include unintentionally and intentionally roughened Si samples and are shown to be consistent with the commonly accepted Si oxidation model.

I. INTRODUCTION

As semiconductor devices are scaled to submicron dimensions in ultra-large-scale integrated (ULSI) circuits, ultrathin SiO$_2$ films less than 10 nm thick are required. In this oxide thickness regime, the interface is a substantial fraction of the device. It is crucial to control the atomic scale structure of the Si/SiO$_2$ interface, because for example, for tunneling even a small degree of interfacial microroughness or nonuniformity can significantly alter device performance. Much work has been done to investigate the Si/SiO$_2$ interface by different techniques, such as transmission electron microscopy (TEM),[1,2] low-energy electron diffraction (LEED),[3] ellipsometry,[4–8] etc., but many details about the interface remain unclear. In the present research, the interface is studied by a novel interface sensitive technique, spectroscopic immersion ellipsometry (SIE).[9–12] Atomic force microscope (AFM) is also used to provide an independent assessment of roughness.

There are several different ways to study the interface region between film and substrate. One way is by using spectroscopic ellipsometry in air or vacuum ambients, as shown in Fig. 1(a). The disadvantage of this method is that an accurate characterization of the ultrathin interfacial transition layer is complicated by the inability to discriminate the optical contributions of the relatively thick overlayer and the thin transition layer by the measured ellipsometric parameters. Alternatively, one can remove the overlayer physically or chemically and then probe the interface, as shown in Fig. 1(b). However, this method could alter the interface region. Addressing these shortcomings, we have developed the SIE technique, which uses a transparent liquid ambient that refractive index matches to the film thereby eliminating the optical response of the overlayer, as shown in Fig. 1(c). Hence, this technique "optically" removes the overlayer and thus enhances the sensitivity to the interface properties. We have shown that the sensitivity is increased more than tenfold using a liquid ambient.[9]

In our previous research, we investigated the evolution of the Si/SiO$_2$ interface as a function of high-temperature annealing (750–1000 °C) by SIE[10] and used the interface model shown in Fig. 2, which is also applicable to this study. Essentially, an interface layer of thickness L_{inf} is covered with a pure SiO$_2$ overlayer of thickness L_{ov} and with SiO$_2$ optical properties. The interface layer is composed of Si protrusions of radius R, separated by a distance D, and covered with a suboxide, SiO$_x$, of thickness L_{SiO} so that $L_{inf}=R+L_{SiO}$. The modeled data in terms of L_{inf} show a shrinkage of the interface with annealing. Distinct modes of behavior were observed for the evolution of the interface. For short annealing times a rapid change in the interface is observed that correlates with the disappearance of protrusions R, followed by a slower change that correlates with the disappearance of the suboxide, L_{SiO}. At high annealing temperatures we believe that viscous relaxation dominates,[13] while at low annealing temperatures L_{SiO} reduction is apparent. These interface changes were studied using about the same thickness, 17 nm, of thermally grown SiO$_2$ film at 800 °C in dry O$_2$.

In the present work, we further investigate the interface changes associated with different Si orientations and for different SiO$_2$ thicknesses. Also, to verify our model and the observation that R is changing, we purposely roughened the Si surface and used SIE and AFM, to assess roughness changes.

II. EXPERIMENTAL PROCEDURES AND DATA ANALYSIS

Single crystal (100), (110), and (111) oriented 2 Ω cm p-type silicon wafers were cleaned using a slightly modified RCA procedure[14] and thermally oxidized at 800 and 1000 °C in a fused silica furnace tube in clean dry oxygen to grow SiO$_2$ thicknesses from about 5 to 100 nm. A commercially available vertical ellipsometer bench was modified to become a rotating analyzer spectroscopic ellipsometer.[15] A special fused silica immersion cell has been designed for the
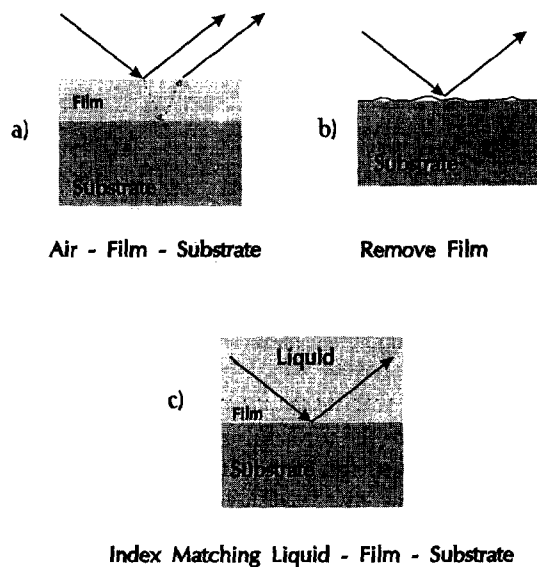
FIG. 1. Methods to analyze an interface: (a) optically with overlayer in place; (b) remove overlayer; and (c) immersion, where overlayer is optically removed (after Ref. 10).

SIE measurements.[11] The key feature of the cell is that its windows are fixed normal to the incident light, in order to prevent a change in beam direction when the light enters the liquid medium. Generally, it is difficult to achieve a perfect refractive index match between the liquid ambient and the SiO₂ overlayer over a broad spectral range. Therefore, small deviations are accounted for in the analysis. Carbon tetrachloride (CCl₄) is a suitable immersion liquid for index matching to SiO₂ films. The index for CCl₄ was calculated using the Cauchy dispersion formula and values used with details previously discussed.[9-12] The CCl₄ used was reagent

FIG. 2. Interface model (after Ref. 10).

grade and the residue after evaporation is smaller than 0.000 01%. We tested whether the SiO₂ surface is altered by exposure to CCl₄ either by precipitation of impurities at the surface or penetration of CCl₄ in SiO₂ and occlusion. Long time exposure showed no changes and with room-temperature drying after CCl₄ exposure the SiO₂ properties were restored.

As mentioned above, our working model for the interface between crystalline Si substrate and amorphous SiO₂ film is shown in Fig. 2. The transition region has a structure with two major components: the "physical" interface and the "chemical" interface. The physical interface is represented by microroughness or protrusions of Si into the oxide. The chemical interface consists of a suboxide, SiO_x, with $0 < x < 2$. We describe the crystalline silicon protrusions as hemispheres with an average radius R, which form a hexagonal network with an average distance D between centers. For unetched samples $D = 4.5$ nm was used in accord with previous results and literature agreement.[10] For etched samples $D = 740.0$ nm was used and this value was taken from AFM measurements which follow. The protrusions and the region between them are covered by a layer of suboxide assumed to be SiO (i.e., $x = 1$) with an average thickness L_{SiO}, and an effective interface thickness L_{inf}. The Bruggeman effective medium approximation (BEMA) was used to calculate the effective dielectric function of the interface.[16] The refractive index for thin SiO₂ films was obtained from the Sellmeier approximation and for thick SiO₂ and Si from the literature. The dielectric function for SiO_x with $x = 1$ was calculated using the BEMA assuming that SiO_x is a mixture of a-Si and SiO₂. The procedures, formulas, values used, and references were previously published.[9,10] Ellipsometry is an optical technique used for the characterization of a bare or film covered surface and is based on exploiting the polarization transformation that occurs as a beam of polarized light is reflected from or transmitted through the interface or film.[17] The measured wavelength (λ) dependent ellipsometric quantity, $\rho(\lambda)$, at the incident angle ϕ is called the complex reflectance ratio and defined as

$$\rho(\lambda) = (\tan \Psi)e^{j\Delta}, \tag{1}$$

where $\tan \Psi$ is the ratio of the amplitude attenuation, Δ is the total phase shift. The incident angle in our experiment is 72° and the wavelength range is from 330 to 550 nm. In order to obtain unknown interface parameters, we used a Marquardt nonlinear best-fit algorithm which minimizes the value of the error function:

$$\delta = \frac{1}{N}\left[\sum_j^N \left(1 - \frac{\Delta_{i,j}^{cal}(\phi_i, E_j, P)}{\Delta_{i,j}^{exp}}\right)^2 + \left(1 - \frac{\Psi_{i,j}^{cal}(\phi_i, E_j, P)}{\Psi_{i,j}^{exp}}\right)^2\right]^{1/2}, \tag{2}$$

where N is the number of wavelengths and P is a vector of unknown interface parameters, E_j is the photon energy, ϕ_i is the angle of incidence, and the superscripts cal and exp refer
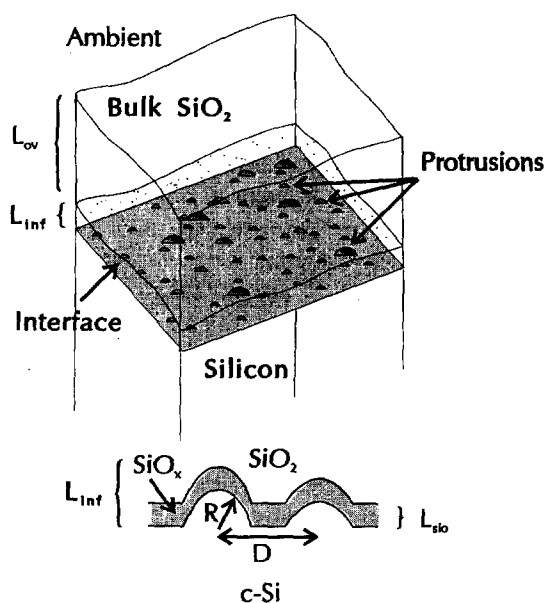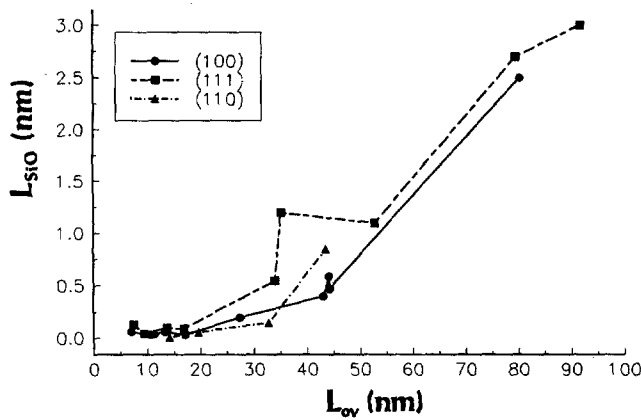
FIG. 3. SIE modeled data in terms of the relationship between the thickness of the layer SiO, L_{SiO}, and the thickness of the SiO₂ overlayer, L_{ov}.
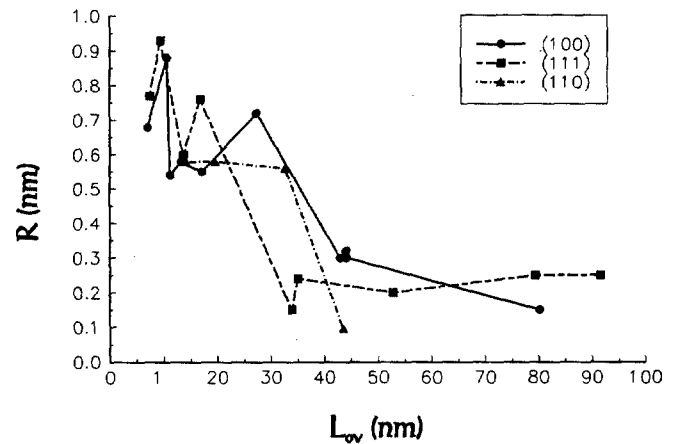

FIG. 4. SIE modeled data in terms of the relationship between the roughness R at the interface and the thickness of the SiO₂ overlayer, L_{ov}.

to calculated and experimentally derived values. Δ^{cal} and Ψ^{cal} are the values obtained using the vector P from expanded Fresnel formulas.

Using a commercially available AFM, rms roughness values were determined for the different samples. Because the roughness values are influenced by tip, scan size, and even scan condition, most of the parameters were kept the same from sample to sample. All tips were checked on standards for x, y, and z calibration prior to imaging. Prior to measurement, all samples were cleaned using a modified RCA procedure, then some samples were purposely roughened by chemical etching using the following solution: HNO₃: HF: CH₃COOH (30:20:40) for 10 and 15 s at room temperature with ultrasonic vibration. The etched samples were first measured by AFM and then thermally oxidized for different times to grow different thicknesses of the SiO₂ overlayer. After SIE measurement, the samples were HF dipped for 10 s and were again measured by AFM. We have studied the effect of HF removal of SiO₂ and found that even up to 1 min in 48% HF the morphological changes in the Si surface were not noticeable by AFM.[18] Thus we believe that the 10 s HF dip will not measurably affect the interface roughness. After etching Si for 10 and 15 s, a root mean square (rms) roughness of about 3 and 6 nm, respectively, is measured and a separation of about 740 nm is obtained and used for D in the interface model. While this induced roughness is greater by more the 3× than that which we see in AFM or SIE on

unetched Si, we believe that this level of roughness is small enough to be relevant, but large enough to be unambiguously measured, while the unetched rough features are at the limit of our AFM measurement.

III. RESULTS AND DISCUSSION

Figures 3 and 4 show the changes of the model parameters, L_{SiO} and R, with oxide thickness and Si orientation for the unetched commercially obtained highly polished Si wafers. Within the experimental and analytical uncertainties, we observe no Si orientation effect, i.e., the three major orientations show the same qualitative and quantitative behavior. It is seen that L_{SiO} increases and R decreases with increasing oxide film thickness L_{ov} which is the extent of oxidation. The interface region L_{inf} increases with L_{ov} owing to the fact that L_{SiO} is typically larger than R for $L_{ov}>50$ nm. The systematic decrease in R and increase in L_{SiO} with increasing SiO₂ film thickness appears real and is in agreement with independent measurements.[19] However, attempts to use AFM to confirm changes in R proved futile, because the level of roughness and the changes seen by SIE are below the error and noise limits of our AFM. Therefore, we also examined purposely etched Si surfaces where the level of roughness can be unambiguously measured by AFM. The values shown in Fig. 3 for L_{SiO} of greater than 0.5 nm for L_{ov} values larger than 30 nm are significantly larger than previously

TABLE I. Comparison of AFM and SIE results after oxidation. Short ox. : 4.5 h, dry oxidation at 800 °C, L_{ov} =38 nm. Long ox. : 12 h, dry oxidation at 800 °C, L_{ov}=70 nm.

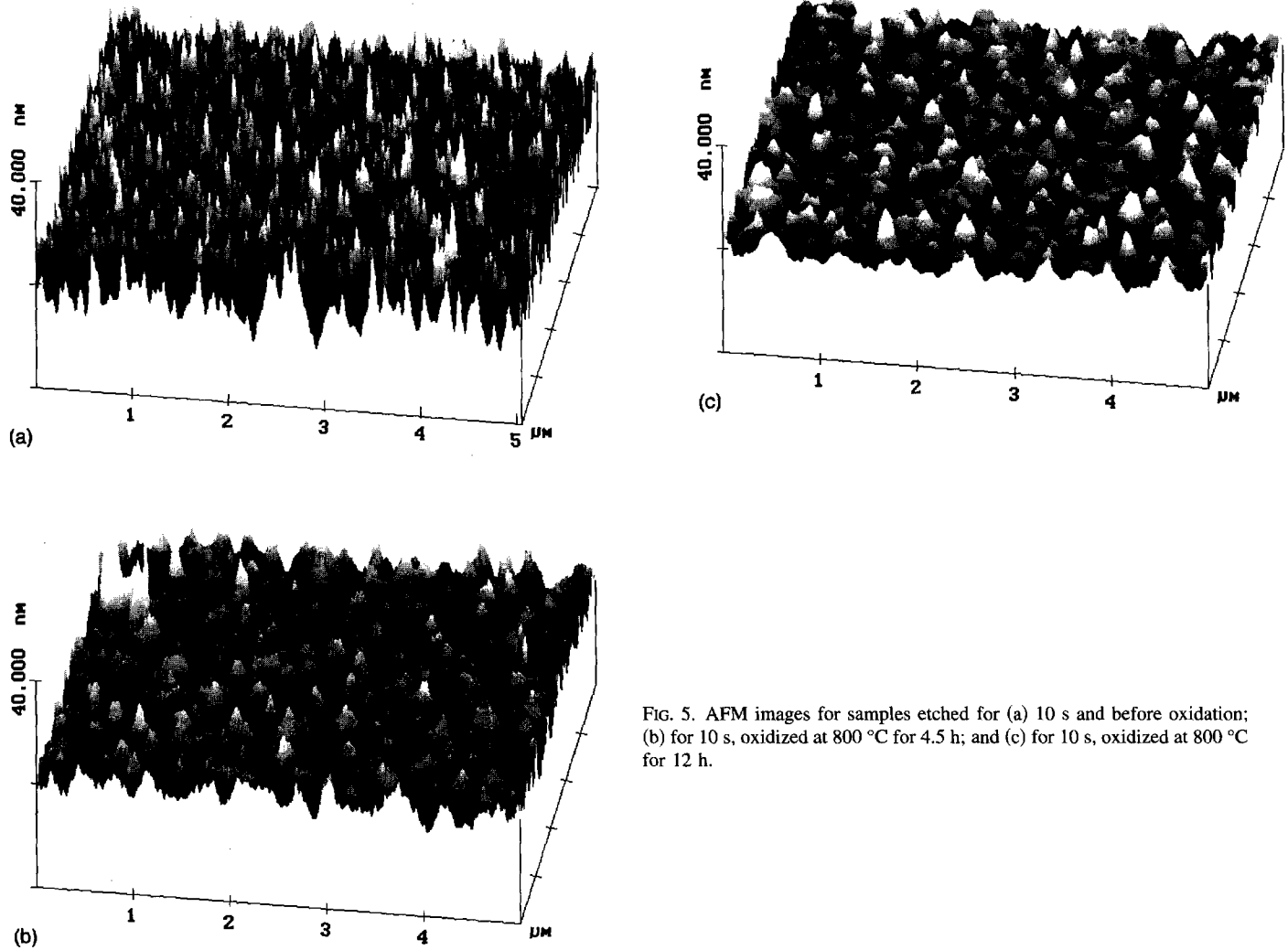| Etching time (s)	Oxidation time (h)	Interface roughness from AFM-rms (nm)		Interface roughness from SIE (nm)	
		Initial	After oxidation	After oxidation	
10	4.5	3.45 ± 0.44	2.20 ± 0.23	7.0 ±0.5	δ=3.09×10⁻²
10	12.0	3.45 ± 0.44	1.69 ± 0.11	5.8 ± 0.5	δ=2.27×10⁻²
15	4.5	6.53 ± 0.30	6.27 ± 0.30	8.8 ± 0.5	δ=1.82×10⁻²
15	12.0	6.53 ± 0.30	4.64 ± 0.49	7.2 ± 0.5	δ=2.19×10⁻²

FIG. 5. AFM images for samples etched for (a) 10 s and before oxidation; (b) for 10 s, oxidized at 800 °C for 4.5 h; and (c) for 10 s, oxidized at 800 °C for 12 h.

reported.[20] Based on the sensitivity and reproducibility of the SIE technique we estimate errors of up to ±0.3 nm in L_{SiO} and ±0.1 nm in R in Figs. 3 and 4. Since the SIE index matches to SiO_2, we do not expect a variation interface sensitivity with L_{ov} as Taft reported[20] and illustrated with extensive etch back experiments. However, to further check this point, we etched back the (100) sample in Fig. 3 from about $L_{ov}=80$ nm with L_{SiO} about 2.5 nm to about $L_{ov}=50$ nm where L_{SiO} was about 2.4 nm confirming both the quality of index matching and the results for L_{SiO}. At this time we are not certain about the origin of this effect, but we believe it to be a chemical effect discussed further below with the Si oxidation model. Based on the following argument we rule out a stress effect. Our previous work[21] has shown an intrinsic interface stress at oxidation temperature of -4.5×10^9 dynes/cm² which would not be substantively relieved at the 800 °C oxidation temperature, and which decreased toward the free SiO_2 surface. Thus the fact that the SiO_2 is thicker would not significantly change the stress-affected interface optical properties. The addition of the compressive thermal stress component when the sample is cooled from 800 °C to room temperature does not change the argument, since this is

a constant. The force on the oxide due to thickness does increase with thickness, but considering a stress gradient, we believe this to be a small effect.

The results from purposely roughened Si surfaces are shown in Table I which includes the root mean square (rms) roughness results from AFM along with the results of the interface roughness from SIE. AFM was performed at three positions on each sample with an initial rms roughness of about 3.5 nm for the 10 s etch and with an initial rms roughness of about 6.5 nm for the 15 s etching. These samples were oxidized for both 4.5 h (short time) and 12.0 h (long time) at 800 °C and AFM was performed after HF etch. In both cases, the roughness decreased. AFM and SIE show parallel deceases in roughness after oxidation, giving credence to the ability of the SIE measurement and modeling to follow the changes at the interface. The rms values from AFM and the SIE values are different with the SIE values yielding the larger R. The rms value should be about 1/2 the peak to valley height of protrusions. The after oxidation AFM and SIE measurements give this order and considering that the measurements are fundamentally different, with AFM being a local measurement, and ellipsometry

TABLE II. Comparison of AFM and SIE results for different oxidation temperatures.

Oxidation temperature (°C)	SiO₂ thickness (nm)	R from AFM-rms (nm)	R from SIE (nm)	L_{SiO} from SIE (nm)
1000	24.8	2.45 ± 0.45	5.8 ± 0.5 $\delta = 3.02 \times 10^{-2}$	0.7 ± 1.0
800	28.2	2.74 ± 0.40	6.0 ± 0.5 $\delta = 1.28 \times 10^{-2}$	3.7 ± 1.0

averages the optical response of a relatively huge area, the agreement is gratifying. The changes in the Si surface topology upon oxidation as observed by AFM, are shown in Fig. 5. From prior to oxidation [Fig. 5(a)] to short (4.5 h) and long (12.0 h) oxidation [Figs. 5(b) and 5(c)], a decrease in both height and shape of the Si protrusions is observed. Interface studies were also performed on samples grown at different oxidation temperatures, but to similar thickness. These samples were etched by the same solution as above for 11 s. The roughness results from AFM and SIE in Table II, are again, in reasonable concordance and show that they have similar interface roughness.

The SIE and AFM results are consistent with the well-accepted linear-parabolic (LP) Si oxidation model[22] which yields an accurate representation of the growth of SiO₂ on Si over a wide range of oxide thickness, temperature, and oxidant partial pressures.[23] According to the LP model, the relationship between film thickness L and oxidation time t is

$$t - t_0 = \frac{(L - L_0)}{k_l} + \frac{(L^2 - L_0^2)}{k_p},\tag{3}$$

where the linear k_l and parabolic k_p rate constants are given as

$$k_l = \frac{C_1 k}{\Omega}, \qquad k_p = \frac{2DC_1}{\Omega},\tag{4}$$

where $\Omega = 2.3 \times 10^{22}$ cm⁻³, k is the reaction rate constant, D the oxidant diffusion coefficient, the subscript 0 denotes the initial values, and C_1 is the concentration of oxidant at the Si surface.

For long oxidation times, Eq. (3) reduces to: $t \cong L^2/k_p$. This is termed the parabolic growth law and implies that oxide growth is diffusion controlled. In other words, as the oxide layer thickens, the oxidizing species must diffuse a longer distance to the Si/SiO₂ interface and as oxidation continues the concentration of oxygen drops at the interface. The reaction thus becomes limited by the rate at which the oxidizing species diffuse through the oxide. It was shown that at elevated temperatures and with an oxygen deficiency, SiO₂ decomposition takes place:

$$\text{SiO}_2 + \text{Si} \rightarrow 2\,\text{SiO}.\tag{5}$$

The oxide decomposition reaction is initiated at active defect sites already present at the Si/SiO₂ interface.[24] Based on the Kelvin equation,[25] which teaches that the thermodynamic activity is higher for regions of smaller radius of curvature, the Si protrusions in our model may be considered as

defects that could initiate the SiO₂ decomposition. Our results show that with the thickening of the SiO₂, the thickness of the SiO layer, L_{SiO}, at the interface increases and at higher oxidation temperatures L_{SiO} is smaller (see Table II) due to the enhanced diffusivity of oxidant. That the average radius of the crystalline protrusions R decreases can also be explained using the linear-parabolic model. In the early stage of oxidation, the kinetics are under interface control and the sharp protrusions would oxidize fastest, thereby smoothing the surface. In the diffusion region the Si surface is less important and the change in R should be less. Figure 4 shows that after 30 nm the change in R levels.

IV. CONCLUSION

Using SIE we found that increased thermal oxidation reduced interface roughness and increased the suboxide layer thickness. These results were confirmed by AFM on purposely roughened Si surfaces. No differences were seen for the three major Si orientations or at oxidation temperatures of 800 and 1000 °C in dry O₂. The results are concordant with the commonly accepted linear-parabolic oxidation model.

ACKNOWLEDGMENT

[1]A. H. Carim and R. Sinclair, Mater. Lett. **5**, 94 (1987).

[2]N. M. Ravindra, D. Fathy, J. Narayan, J. K. Srivastava, and E. A. Irene, J. Mater. Res. **2**, 216 (1987).

[3]P. O. Hahn and M. Henzler, J. Appl. Phys. **52**, 4122 (1981).

[4]E. Taft and L. Cordes, J. Electrochem. Soc. **126**, 131 (1979).

[5]D. E. Aspnes and J. B. Theeten, J. Electrochem. Soc. **127**, 1359 (1980).

[6]A. Kalnitsky, S. P. Tay, J. P. Ellul, S. Chongsawangvirod, J. A. Andrews, and E. A. Irene, J. Electrochem. Soc. **137**, 234 (1990).

[7]V. Nayar, C. Pickering, and A. M. Hodge, Thin Solid Films **195**, 185 (1991).

[8]G. E. Jellison, Jr., J. Appl. Phys. **69**, 7627 (1991).

[9]V. A. Yakovlev and E. A. Irene, J. Electrochem. Soc. **139**, 1450 (1992).

[10]V. A. Yakovlev, Q. Liu, and E. A. Irene, J. Vac. Sci. Technol. A **10**, 427 (1992).

[11]Q. Liu and E. A. Irene, Mater. Res. Soc. Symp. Proc. **315**, 405 (1993).

[12]E. A. Irene and V. A. Yakovlev, *The Physics and Chemistry of SiO₂ and the Si–SiO₂ Interface*, edited by C. R. Helms and B. E. Deal (Plenum, New York, 1993).

[13]E. A. Irene, E. Tierney, and J. Angillelo, J. Electrochem. Soc. **129**, 2594 (1980).

[14]W. Kern and D. A. Puotinen, RCA Rev. **31**, 187 (1970).

[15]X. Liu, J. W. Andrews, and E. A. Irene, J. Electrochem. Soc. **138**, 1106 (1991).

[16]D. E. Aspnes, Thin Solid Films **89**, 249 (1982).

[17]R. M. A. Azzam and N. W. Bashara, *Ellipsometry and Polarized Light* (North-Holland, Amsterdam, 1977).

[18]J. C. Poler, K. K. McKay, and E. A. Irene, J. Vac. Sci. Technol. B **12**, 88 (1994).

[19]T. Hattori, H. Nohira, Y. Tamura, and H. Ogawa, Jpn. J. Appl. Phys. **31**, (1992).

[20]E. Taft and L. Cordes, J. Electrochem. Soc. **126**, 131 (1979).

[21]E. Kobeda and E. A. Irene, J. Vac. Sci. Technol. B **6**, 574 (1988); **7**, 163 (1989).

[22]B. E. Deal and A. S. Grove, J. Appl. Phys. **36**, 3770 (1965).

[23]E. A. Irene, CRC Crit. Rev. Solid State Mater. Sci. **14**, 175 (1988).

[24]G. W. Rubloff, K. Hoffmann, M. Liehr, and D. R. Young, Phys. Rev. Lett. **58**, 2379 (1987).

[25]A. W. Adamson, *Physical Chemistry of Surfaces* (Wiley, New York, 1982).